Sensors International 6 (2025) 100324

Contents lists available at ScienceDirect

Sensors International

journal homepage: www.keaipublishing.com/en/journals/sensors-international

A smart glove to evaluate Parkinson's disease by flexible piezoelectric and inertial sensors

R. De Fazio [a], C. Del-Valle-Soto [b], V.M. Mastronardi [a,c], M. De Vittorio [a,c], P. Visconti [a,c,*]

[a] Department of Innovation Engineering, University of Salento, Road to Monteroni, Building 'O', Lecce, 73100, Italy
[b] Facultad de Ingeniería, Universidad Panamericana, Álvaro Del Portillo 49, Zapopan, 45010, Mexico
[c] Center for Biomolecular Nanotechnologies, Italian Technology Institute IIT, Via Eugenio Barsanti, 14, Arnesano, 73010, Lecce, Italy

ARTICLE INFO

Keywords:
Parkinson's disease
MDS-UPDRS scale
Aluminum nitride
Inertial sensors
Machine learning

ABSTRACT

Parkinson's disease (PD), to date, is widespread. It is a neurodegenerative disease that impairs the quality of life of the affected, as it is a slowly but progressively evolving disease. This paper presents a smart glove for evaluating PD patients by monitoring hand tremors and evaluating specific exercises involved by the MDS-UPDRS (Movement Disorder Society - Unified Parkinson Disease Rating Scale), enabling disease evolution assessment. The smart glove consists of a TPU flexible support, integrating two flexible MEMS piezoelectric sensors based on Aluminum Nitride and an inertial sensor to detect finger and arm movements. The smart glove integrates an electronic conditioning section for piezoelectric signals to make them suitable for the following acquisition by a microcontroller section based on nRF52840 SoC, which jointly processes the piezoelectric and inertial signals related to standard patient's hand and arm exercises (i.e., finger tapping, fist opening/closing of the hand, resting hand tremor), assigning them scores according to the MDS-UPDRS. Three embedded Machine Learning (ML) algorithms based on Neural Networks (NN) were deployed to classify piezoelectric and inertial signals. Seven individuals, six of them with diagnosed PD, were involved in developing ML models. Datasets were gathered to train and test the ML algorithms, constituted by signal samples related to three tests involved in the UPDRS scale according to PD severity. The tests demonstrated the proper operation of the proposed smart glove in tracking the movement changes induced by PD; also, the developed embedded ML algorithms showed performance in classifying hand/arm movements, reaching 95.12 %, 98.39 %, and 96.62 % for finger-tapping, hand-fist closure, and resting tremor, respectively.

1. Introduction

Parkinson's Disease (PD) was first described in 1817 by the British physician James Parkinson. Motor function disorders, such as bradykinesia (i.e., slowness of movement), akinesia (i.e., impaired voluntary movement), rigidity, and tremor, are induced by the degeneration of these neurons [1]. Unfortunately, there is no known cure for PD, and the drugs available can help but only allow a reduction of symptoms; therefore, to manage the pathology, it is important to monitor the patient's motor disorder and his neurophysiological signals accurately. Remote monitoring systems, continuous over time and easy to use, could positively impact the health of the people involved and the management of clinical trials. Through wearable devices, the specialist doctor could better understand the disease and all its nuances more effectively than the sporadic controls and self-assessment [2,3]. Multiple methods for diagnosing and monitoring PD have been described in the scientific literature using accelerometers, gyroscopes, or EMG sensors to evaluate the kinetic properties or muscle activity of various body areas [4–6]; also, triboelectric nanogenerators (TENGs) provide an additional option for continuous PD monitoring because they are comfortable and stretchable. A. Vera et al., in Ref. [7], reported a triboelectric nanogenerator to monitor PD based on Ecoflex™ and PEDOT: PSS. The sensor is placed on the forearm to detect hand movements (e.g., tremors, finger tapping, rigidity). It was included in a wearable sensor to evaluate PD problems and moderate slowing problems [8]. Also, N. Kim et al. developed a stretchable TENG to monitor PD using catechol, chitosan, and diatom from the ocean [9]. The Catechol-Chitosan-Diatom Hydrogel (CCDHG)-TENG was deposited on M-shaped Kapton support. The

* Corresponding author. Department of Innovation Engineering, University of Salento, Road to Monteroni, Building 'O', Lecce, 73100, Italy.
E-mail addresses: roberto.defazio@unisalento.it (R. De Fazio), cvalle@up.edu.mx (C. Del-Valle-Soto), vincenzomariano.mastronardi@unisalento.it (V.M. Mastronardi), massimo.devittorio@unisalento.it (M. De Vittorio), paolo.visconti@unisalento.it (P. Visconti).

https://doi.org/10.1016/j.sintl.2024.100324
Received 25 June 2024; Received in revised form 12 October 2024; Accepted 17 December 2024
Available online 18 December 2024
2666-3511/.

resulting sensor is applied to the patient's wrist, processing the voltage signal by an ML algorithm to determine the state of the PD patient. Also, inertial sensors can be used to evaluate PD patients' condition. M. Heijmans et al. in Ref. [10] used three inertial sensors, each containing an accelerometer and a gyroscope, placed around the wrists and on the chest. These sensors gathered tremor data and compared it with those provided by the ESM (Experience Sampling Method) questionnaires provided to the PD patient during the day to verify the reliability and smooth operation of the sensors. In addition, S. Sajal et al. combined rest tremor and voice degradation by collecting data remotely utilizing smartphones and employing a cloud-based machine learning system for telemonitoring PD patients [11]. Also, M. Yousef et al. proposed a wearable device for tremor detection using three different storage and monitoring modalities, i.e., offline, online, and live monitoring [12].

Piezoelectric and piezoresistive transducers can detect hand and finger movements. A. Batra et al. presented a low-cost, lightweight metal ring with a PVDF piezoelectric transducer [13]. Intentional rhythmic and random tremors were used to test the performance of their prototype piezo-ring. Amplitude and frequency are easily extracted from the waveform seen on the oscilloscope. Furthermore, amplitude and signal energy may be extracted from frequency spectra and used as a tremor severity metric. Finally, a multimodal smart glove for PD assessment was presented in Ref. [14]. The glove comprises bending and pressure sensors, as well as an IMU (Inertial Measurement Unit). Sensor's data were classified through K-Means and Back Propagation Neural Networks to classify muscle strength and tremor, achieving 95.38 % accuracy. In addition, in Ref. [15], the authors developed a smart glove including piezoresistive and inertial sensors to remotely assess the motor symptoms of PD. Indeed, the device includes three flexure sensors and an IMU to detect finger and arm movements during the execution of six standard exercises associated with the MDS-UPDRS-III. The data acquired by the glove are shared by MQTT with a local gateway, where data are processed to extract useful features for quantifying the disease severity.

This paper presents a compact and non-invasive smart glove based on advanced and commercial sensors to evaluate PD severity. The device consists of flexible support to be applied to the hand equipped with piezoelectric and inertial sensors to acquire and process on board the data related to the hand tremor using sensors, providing direct indexes indicating the patient's condition (Fig. 1). In detail, the device relies on highly flexible and thin piezoelectric sensors based on Aluminum Nitride (AlN), whose manufacturing process is patented by the Italian Institute of Technology (IIT), featured by high sensitivity in detecting body movements [16,17]. Two piezoelectric sensors are integrated into the flexible support: one near the junction between the thumb and index finger, the other near the index finger. Neurologists diagnose and evaluate PD based on the patient's medical records, a visual inspection of their movements, and additional evaluation using the Unified Parkinson's Disease Rating Scale (UPDRS). C. Goetz et al., in Ref. [18], introduced the MDS-UPDRS method, describing its function and structure; this scale has four parts: Part I deals with "non-motor experiences of daily living", Part II concerns "motor experiences of daily living", Part III regards "motor examination", and Part IV the "motor complications". Concerning hand movement disorders, the clinic assessment involves some physical tests, examined based on visual analysis, to which a score is assigned. Our system considers three standard tests associated with the MDS-UPDRS-III to evaluate PD patients: finger tapping, hand fist closure, and resting tremor. The piezoelectric and inertial signals are acquired and processed by glove and classified using embedded Machine Learning (ML) algorithms for scoring the PD patient. Test results are sent, processed, and stored in a digital record on a cloud platform, allowing neurologists to monitor the patient's course easily. The device allows the PD patient to perform the tests alone at home, enabling the neurologist to access it remotely also making the assessment more objective and effective than a visual one.

2. Material and methods

2.1. Architecture of the proposed smart glove

The proposed wearable device relies on a flexible glove wrapped around the hand back, palm, and index finger-thumb junction, that includes two AlN-based piezoelectric sensors [16,17]. One

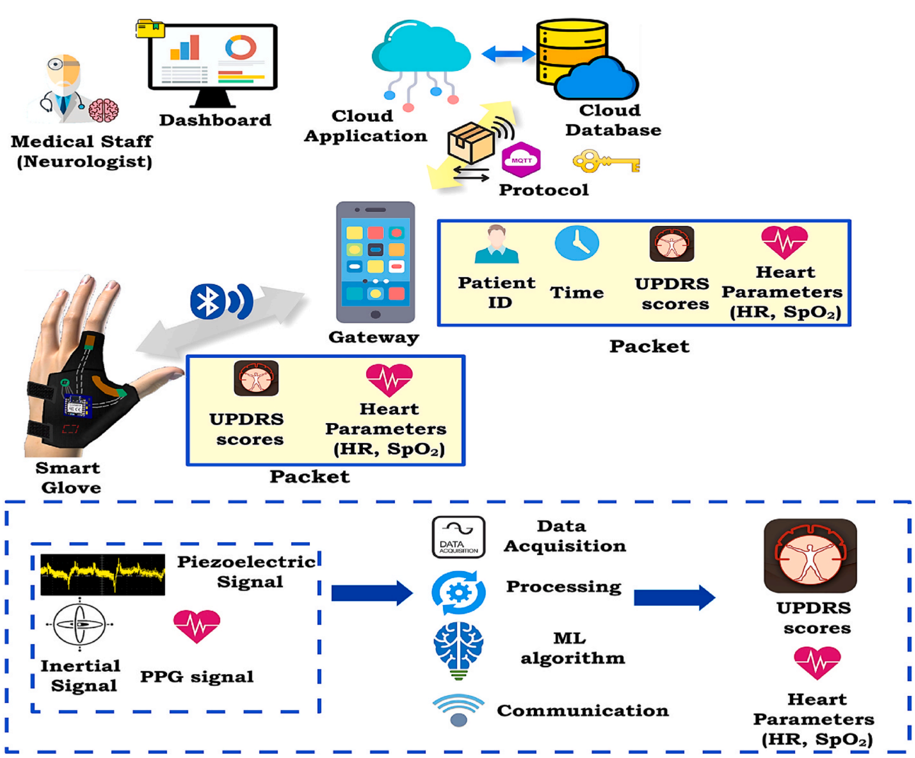

Fig. 1. Graphical representation of the monitoring system for Parkinson's patients based on the proposed smart glove.

half-moon-shaped sensor is placed between the thumb and index finger, while the second rectangular-shaped sensor is placed on the back close to the index finger. The two piezoelectric sensors made by a manufacturing process patented from IIT are characterized by the following specifications: 0.012 V $Pa^{-1}m^{-2}$ and 0.017 V $Pa^{-1}m^{-2}$ sensitivity, 3.6 10^{-9} V^2 and 3.9 10^{-9} V^2 noise level, 20 mm × 10 mm × 26 μm and 32 mm × 10 mm × 26 μm dimensions, for the rectangular- and half-moon-shaped sensors, respectively [16,19]. Also, they are highly resilient and stable in performance, making them suitable for this application. The PD's hand tremor is usually defined as a "Pill-Rolling" tremor, where the thumb and forefinger appear to roll something, like a small pill, between them [20]. Thus, the position of the two piezoelectric sensors was selected based on the study of areas mainly involved in this characteristic tremor to maximize the applied solicitation and, thus, their response; also, their shape has been carefully evaluated to better adapt to the anatomical area and, therefore, improve mechanical coupling. The sensors were installed into the glove in fixed positions, becoming integral with it and realizing inserts through which the U-FL (Ultra Miniature Coaxial) connectors can pass. Therefore, by wearing the device, the positions of the sensors will remain almost fixed on the patient's hand, ensuring high repeatability of the generated signals. Both sensors can capture hand and finger tremors, generating an output signal that may be analyzed to acquire information about the health status of a patient with PD. The raw signals from the two sensors are input to a low-power conditioning block, which provides the conditioned signals acquired by the nRF52840 SoC (System on Chip) (manufactured by Nordic Semiconductor Inc.) integrated on a Seeeduino XIAO BLE board. Also, the nRF52840 SoC is interfaced with the LSM6DS3 6-axis IMU (manufactured by STMicroelectronics Inc.), enabling acquiring data related to hand movements and tremors. The IMU features 16-bit resolution, configurable full-scale for accelerometer (±2/± 4/± 8/± 16 g) and gyroscope (±125/± 250/± 500/± 1000/± 2000 dps-degrees per second), 3.3 V supply voltage (typical value), compact footprint (2.5 mm × 3 mm × 0.83 mm), and compatibility with SPI and I^2C serial interfaces. The inertial sensor is placed on the hand on the back of the hand to detect hand and arm movements.

The nRF52840 microcontroller acquires data from the interfaced sensors and pre-processes them (i.e., de-trending, digital filtering, envelope extraction, etc.) and elaborates them to evaluate the progress of Parkinson's disease. In particular, based on the evaluation of acquired data, UPDRS scores (from 0 to 4) are provided as an output to the system, which allows for quantifying the degree of severity and progress of the disease. In particular, evaluating the patient involves executing predefined exercises and monitoring limb movements over a given time window, according to the modalities defined by the MDS-UPDRS scale. The scores are a function of the intensity, constancy over time, and frequency of the tremor acquired from the piezoelectric and inertial sensors [21]. The acquired data related to hand and finger movements are processed through embedded ML algorithms based on NN, as detailed in Section 5. Three tests were performed by the smart glove: finger-tapping, fist opening/closing, and resting hand tremor). The device also comprises an MAX30102 PPG (Photoplethysmographic) sensor integrated into the wrist to measure heart rate (HR) and blood oxygenation (SpO_2). These parameters provide useful information about the condition of the cardio-respiratory system; HR monitoring is important for PD patients since the disease damages the automatic nervous system, inducing bradycardia, namely a slowing of the heartbeat compared to the normal heart rate [22]. Also, heart rate variability (HRV) can be estimated from the PPG signal, also providing information on the status of the automatic nervous system; in PD patients, a reduction of HRV occurs with the disease advancement due to impaired parasympathetic regulation [23].

Data are periodically transmitted via Bluetooth by the nRF52840 built-in transceiver to a PC or smartphone, which acts as a gateway (Fig. 2). It collects data, arranges it into packets containing a patient ID, its UPDRS scores, and a timestamp, and forwards it toward the cloud platform via the MQTT (Message Queue Telemetry Transport), where data is displayed on a dashboard, stored and classified according to the patient's ID. The data is sorted into different files according to the patient's ID; each patient will have their medical record. A 370 mAh lithium battery feeds the entire electronic section; the BQ25101 battery management chip (manufactured by Texas Instruments Inc.), integrated

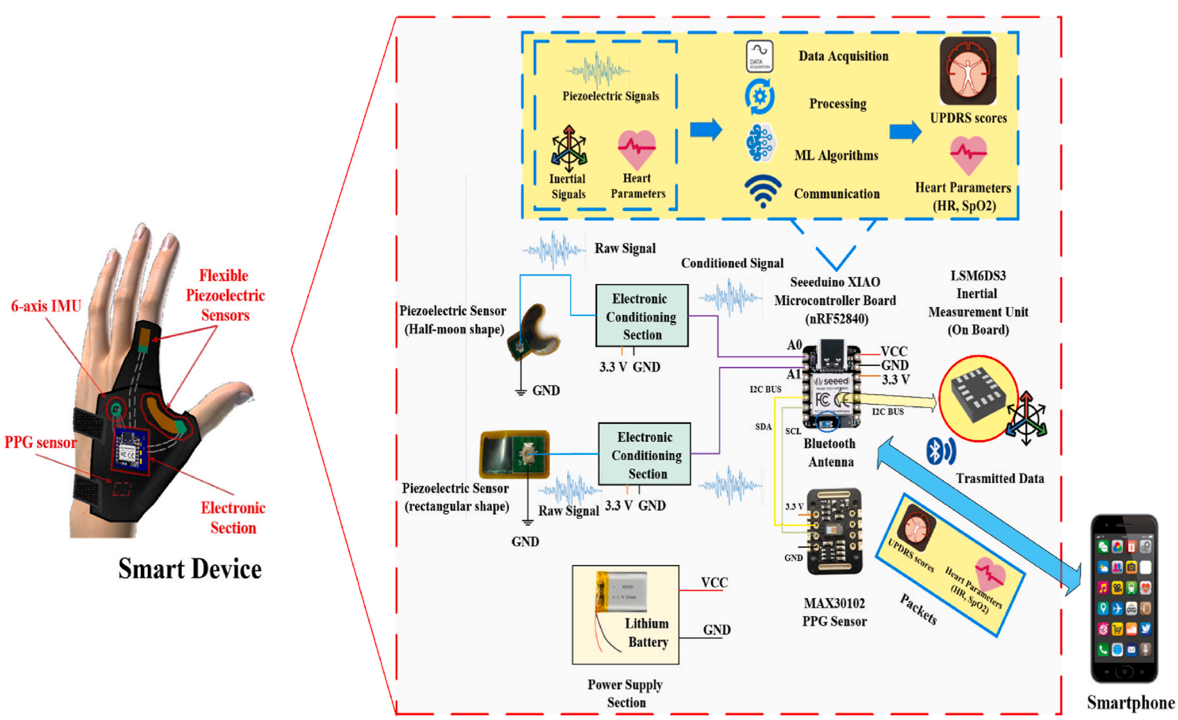

Fig. 2. Block diagram of the smart glove with highlighted main components and functionalities: a dual-channel system with conditioning block, interfacing the piezoelectric sensors with Seeeduino XIAO microcontroller board.

into the Seeeduino board, enables its recharging through the USB cable. Furthermore, the XC6206P332 MR (manufactured by Torex Sem. Inc.) voltage regulator derives +3.3V from the battery to supply the different system components.

2.2. Conditioning section for AlN-based piezoelectric sensors

As mentioned above, two piezoelectric sensors are integrated into the flexible support, each of which converts the mechanical deformation induced by finger and hand movements into a voltage signal; therefore, a dual-channel electronic board was deployed for signal and conditioning, featured by low-power and small dimensions (so it can be easily integrated into the wearable device without creating discomfort). The analog front-end of this electronic board comprises two analog channels, each consisting of two amplifier stages: the first is the charge amplifier, which converts the charge generated by the piezoelectric sensor into the corresponding output voltage signal; the second stage is composed of an amplifier and level shifter which amplifies the difference between the signal applied to the input, that is the signal coming from the first stage and that coming from a voltage reference. A block representation of the analog front end is shown in Fig. 3.

The charge amplifiers integrated into the conditioning board are AC-coupled by a 1 μF blocking capacitor to remove the DC component in the input signal, which could saturate the input stage. An input resistance R_I between the piezoelectric sensor and the inverting input is placed to protect the operational amplifier by limiting the current generated by any voltage applied. The charge amplifiers in both channels have a band-pass behavior between 1.4 Hz and 11 kHz with a gain of 5 mV/pC (for the first channel) and 1 mV/pC (for the second). The cut-off frequencies are set by properly sizing the feedback (R_f) and input (R_i) resistors, as well as the feedback capacitance (C_f). The operational amplifier's output values are limited by supply voltages and, to maximize the output variation range, the polarization has been set at the middle of the nominal output range, namely at half the supply voltage. A pair of resistors is used to pick up the supply voltage straightforwardly and cost-effectively; this polarization stage is tasked with providing a fixed reference voltage V_{ref} by means of a voltage buffer (Fig. 3d). The latter stages in Fig. 3b–c are four-resistors difference amplifiers, amplifying the difference between the signals applied to the input terminals. These stages introduce a band-pass gain equal to 10 V/V; thus, the gain of the two channels of the designed front-end is set to 50 mV/pC (first channel) and 10 mV/pC (second channel), respectively. The half-moon-shaped sensor is connected to the first channel of the conditioning board, while the rectangular-shaped one is connected to the second channel. Both sensors are connected to the conditioning board by a miniature RF coaxial cable with U-FL female connectors integrated into the glove's scaffold. The different gains set for the two channels are due to the different operating modes; the rectangular-shaped sensor placed on the index finger is mainly subject to out-of-plane solicitations during hand movements, whereas the half-moon-shaped sensor is subject to in-plane solicitations that determine a lower sensitivity (0.005 V Pa^{-1} m^{-2}) compared to that obtained for out-of-plane solicitations (0.017 V Pa^{-1} m^{-2}). To take into account this difference, a higher gain (50 mV/pC) was set for the half-moon-shaped sensor featured by a lower sensitivity.

2.3. Prototype assembly of developed wearable device

The smart glove prototype was realized using 3D-printed support from Thermoplastic Polyurethane (TPU) filament. The glove has an aperture at the thumb, covers the palm and back of the hand, and extends along the wrist (Fig. 4a). The top edge has three openings for inserting elastic bands (attached to the bottom edge), which can be closed by adhesive Velcro; this allows it to be pulled out and inserted easily. For integrating one of the two sensors at the junction between the index finger and thumb, an "H"-shaped TPU strip was made; a vertical wing is fixed to the glove's inner part; the other one wraps the thumb (Fig. 4a). A 6 mm × 6 mm opening was realized on the strip at the junction, through which the sensor board applied underneath was to be pulled out. Also, a "T"-shaped TPU strip was made to integrate the second sensor on the index finger, making it adjustable to adapt to the size of the index finger. Afterward, the functional blocks constituting the electronic section of the smart glove (i.e., Seeeduino XIAO BLE and dual-channel acquisition and filtering board) were assembled; the functional blocks were assembled on a PCB (*Printed Circuit Board*) with dimensions 75 mm × 44 mm. The assembled electronic board is equipped with connectors for the conditioning section, PPG sensors, and the battery. To contain the electronic section, a plastic case was made of 3D printing; it

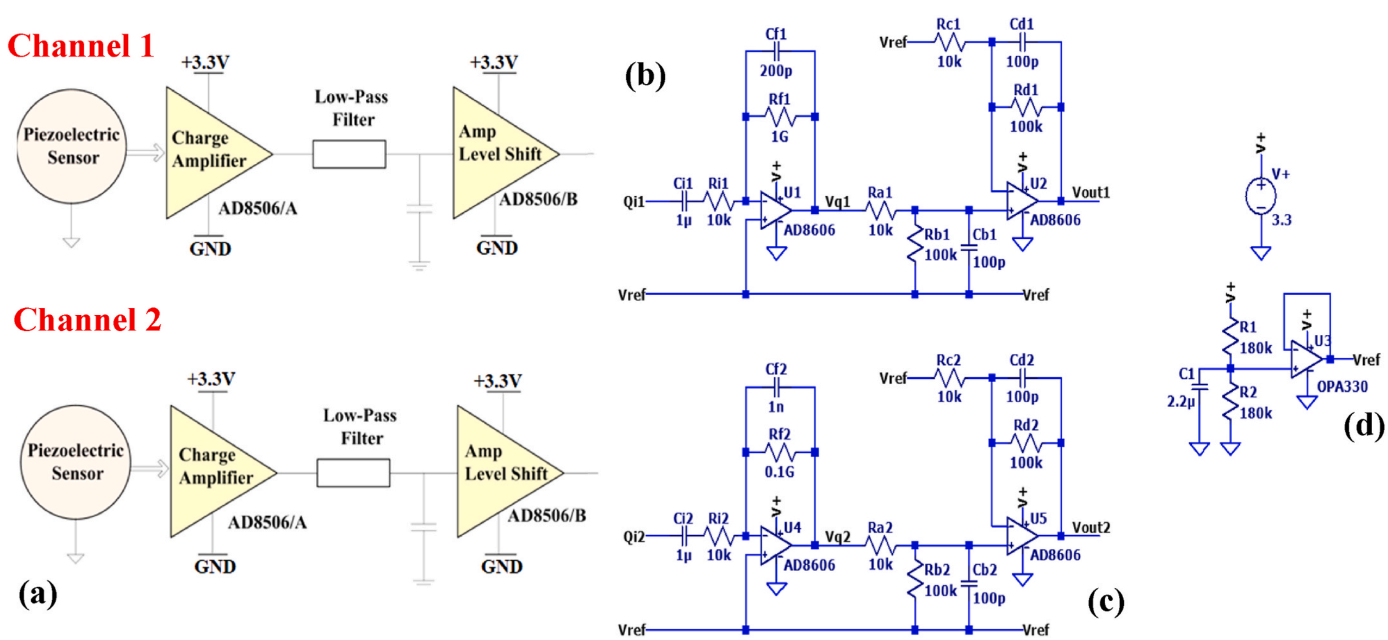

Fig. 3. Block diagram of the dual-channel conditioning board for the piezoelectric sensors integrated into the smart glove (**a**). Schematic of the dual-channel conditioning board for the piezoelectric sensors integrated into the glove: channel 1 (**b**), channel 2 (**c**), and voltage reference (**d**) sections.

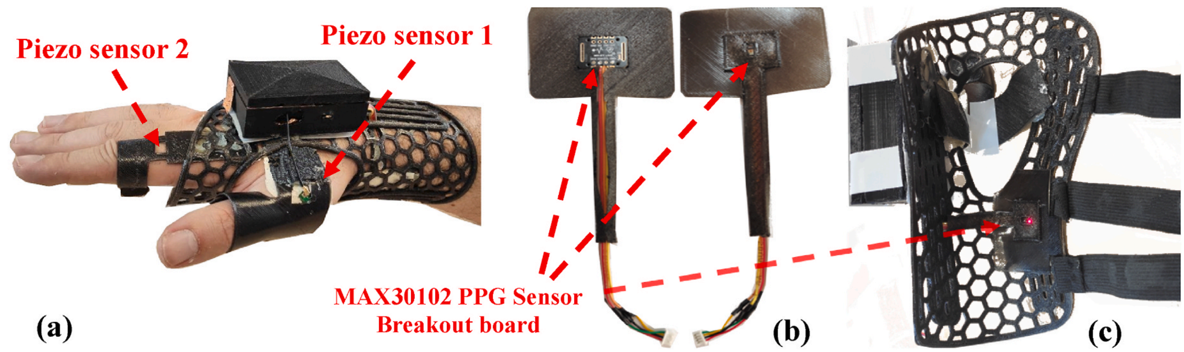

Fig. 4. Fully assembled smart glove: side view (**a**), TPU cover for PPG optical sensor (**b**), and inner view (**c**).

features a curved profile in the underlying part to fit best with the back arching of the hand. Employing Velcro tape, the plastic case was fixed to the flexible support, enabling it to be easily attached/detached. A TPU cover was made using 3D printing to integrate the PPG sensor. This stand consists of the upper part where the sensor is embedded and the lower part with which the cable is covered (Fig. 4b). The realized support lets out the optical section of the PPG sensor, including the red and infrared LEDs and the photodetectors (Fig. 4a). This part was placed on the inside of the glove in contact with the wrist; the cable passes through one of the apertures in the glove and, passing through the corresponding hole on the case, is connected to its connector. The placement of the PPG sensor is shown in Fig. 4c. Fig. 5 shows an example of the signals acquired by the piezoelectric and inertial sensors integrated into the smart glove.

2.4. Description of the involved participants

Seven individuals (4 male and 3 female) were involved in testing the proposed smart glove and developing the ML algorithms to score the PD severity based on evaluating three MDS-UPDRS exercises. The involved subjects are aged between 45 and 76, six of them with PD diagnosed between 5 months and six years ago, assessed according to MDS-UPDRS. In detail, the evaluation distribution for involved subjects is: 1 with Score 1, 2 with Score 2, 1 with Score 3, and 2 with Score 4. Individuals were asked to perform three typical tests associated with the MDS-UPDRS-III (finger tapping, hand-fist closure, and resting tremor) to collect the datasets to train and test the ML models described in Section 3.

3. Results

Three embedded ML algorithms were designed, trained, and tested to support the operation of the developed smart glove, classifying the piezoelectric and inertial signals associated with tests involved in the MDS-UPDRS: finger tapping, hand-fist closure, and resting tremor. The *Edge Impulse* cloud platform was employed to develop the ML algorithms, enabling data acquisition, feature extraction, classifier training and testing, and model deployment to be run on a microcontroller. The models above were trained to classify data from the piezoelectric sensor placed between the thumb and forefinger and inertial data (linear accelerations and angular velocities). In this phase, we want to develop the ML models by considering a single piezoelectric signal and 6-axis inertial signals to reduce the resulting models' memory requirements. Further investigations considering both piezoelectric sensors will be needed in future investigations. The data acquisition was performed using the smart glove, wirelessly transmitting the acquired data to a PC through BLE, which in turn shares it with the *Edge Impulse* platform.

3.1. NN-based algorithm for evaluating finger-tapping exercise

In the finger-tapping exercise, the patient is seated with the elbow resting on a plane; the patient should tap the index finger and thumb ten times as fast and wide as possible (Fig. 6a); based on the speed of execution, the amplitude of the movement, and possible stops and hesitations, a score is associated, indicating the disease severity: 0) smooth movement, 1) 1-2 stops or movement slight slowed or amplitude reduction from 8th touch, 2) 3-5 stops or movement moderately slowed, or amplitude reduction form 5th touch, 3) > 5 stops or movement very slowed, or amplitude reduction form 3rd touch, 4) failure to complete the exercise. A dataset including forty samples of inertial signals and piezoelectric signals with a duration ranging from 14 to 22 s was collected during the finger-tapping tests for each class (i.e., *Score 0*, *Score 1*, *Score 2*, *Score 3*, and *Score 4*), adding *Idle* samples corresponding to the condition in which the arm and hand are steady. Scores were assigned to the dataset samples based on the analysis of the amplitude and temporal characteristics of the signal coming from the piezoelectric sensor, as it is less influenced by extraneous body movements and limb trembling. In particular, if the peak amplitude of the signal is less than 1/8 compared to the amplitude of the first tapping, the movement is considered interrupted; also, a reduction in the amplitude of the signal is less than 30 % of the amplitude of the signal is viewed as a weakening of the movement. Similarly, an increase in the duration of tapping of 20 %, 40 %, and 60 % compared to the initial one for more than three times, the exercise is considered slight, moderate, and very slow, respectively.

Then, the dataset was split into training and test sets (80 %/20 % ratio). A 5-fold cross-validation was used to determine the models' performance before testing. The samples were pre-processed by framing them with 13s time windows and 1s shift to expand the dataset and applying a 6th order low-pass filter with 10 Hz cut-off frequency (Fig. 7); then, spectral features were extracted from the 256-point FFT of sample signals, including statistical features (i.e., RMS-Root Mean Square, skewness, kurtosis), and spectral features (e.g., maximum value). The inference section of the classification chain is a NN constituted by an input layer with 84 features, 3 dense layers of 30, 20, and 10 neurons, respectively, and an output layer with 6 classes (*Score 0*, *Score 1*, *Score 2*, *Score 3*, *Score 4*, *Idle*), was chosen.

3.2. NN-based algorithm for evaluating the hand gesture exercise

In the hand gesture exercise, the patient has the elbow resting on a plane, and the hand is wide open; the exercise consists of opening and closing the hand into a fist 10 times as fast and wide as possible (Fig. 6b). Based on the speed of execution, the amplitude of the movement, and possible stops and hesitations, a score was associated, indicating the disease severity: 0) smooth movements, 1) 1-2 stops or movements slightly slowed, or amplitude reduction from 8th touch, 2) 3-5 stops or movements moderately slowed, or amplitude reduction form 5th touch, 3) > 5 stops or movements very slowed, or amplitude reduction form 3rd

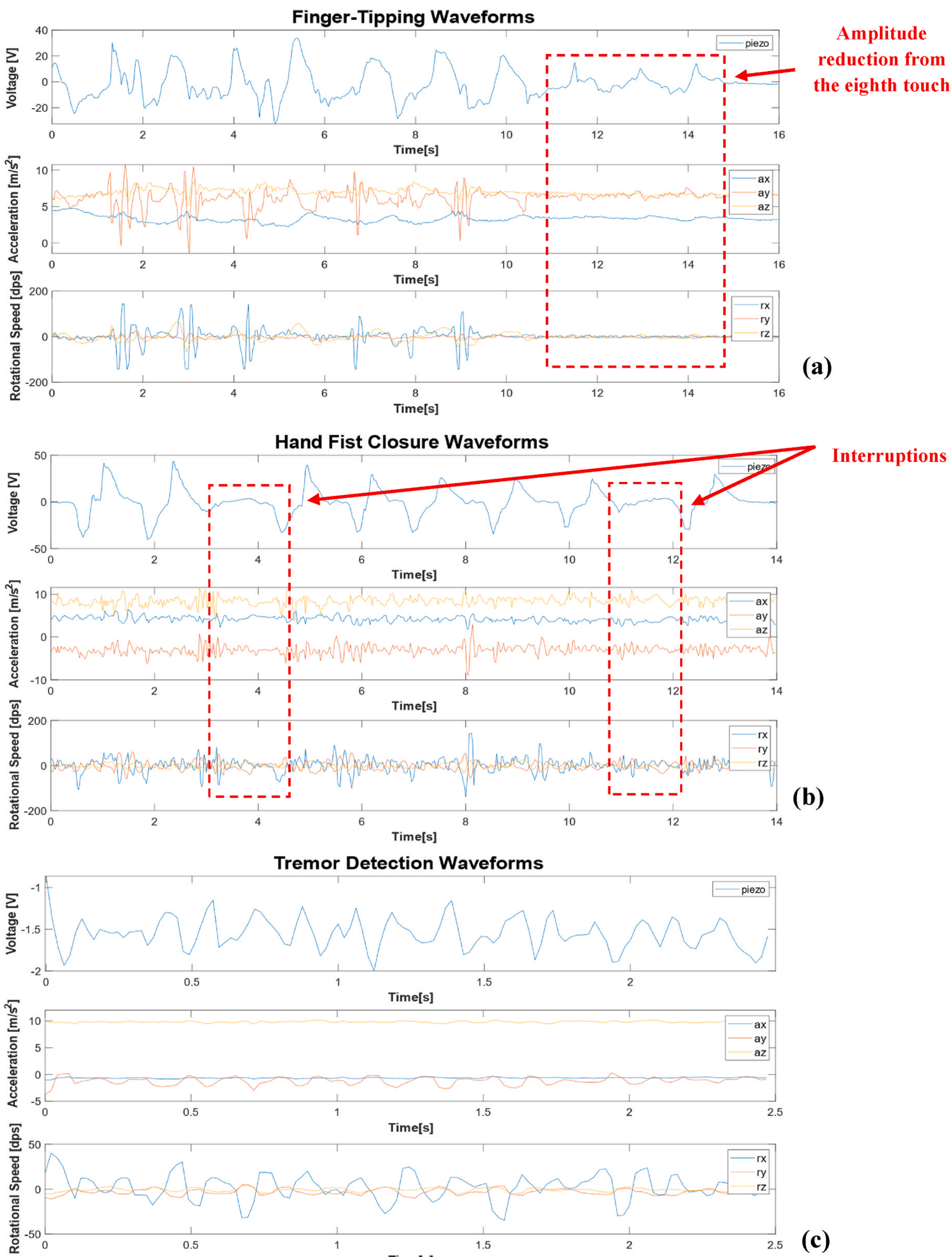

Fig. 5. Piezoelectric and inertial signals acquired by the smart glove during the tests for evaluating PD: Finger-Tapping (*Score 1*) (**a**), Hand-fist closure (*Score 1*) (**b**), Tremor Detection (*Score 1*) (**c**).

touch, 4) failure to complete the exercise.

The criteria to assign a score to the raw data are the same as considered for the finger-tapping exercise and following the definition of the scores reported above. At first, the dataset used for training and testing the ML model was gathered, consisting of forty samples of piezoelectric and inertial signals for each class with a duration in the range of 14–22s, including an *Idle* class, in which the arm and hand are stationary. Similarly to the previous model, the dataset was split into training and test sets according to an 80 %/20 % ratio.

The employed processing chain is similar to the previous one (Fig. 7); a 13 s window size and 1 s shift were set to split the sample signals in frames. These lasts were filtered by an 8th-order low-pass filter with an

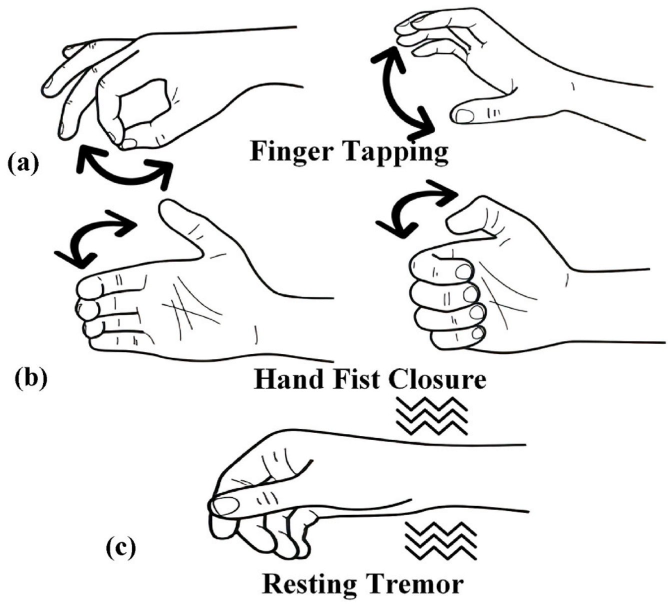

Fig. 6. Execution of the UPDRS tests: (**a**)finger-tapping, (**b**) hand fist closure, and (**c**) resting tremor tests.

8 Hz cut-off frequency before extracting the spectral features from 256-point FFT to train and test the following classifier. The inferring section consists of an NN including an input layer with 112 neurons, three dense layers with 60, 35, and 20 neurons, and an output layer with 6 classes (*Score 0*, *Score 1*, *Score 2*, *Score 3*, *Score 4*, *Idle*), respectively.

3.3. NN-based algorithm for evaluating the hand-resting tremor

The third model asses the resting hand tremor. For proper evaluation, the patient should have his arm stretched out in front of his body, palm facing downward, and fingers well apart (Fig. 6c). Tremor is scored according to the modality defined by MDS-UDPRS, which takes into account its amplitude and constancy over a 10 s window: 0) no tremor, 1) the amplitude <1 cm for 25 % of 10 s window, 2) the amplitude between 1 and 3 cm for 50 % of 10 s window, 3) the amplitude between 3 and 10 cm for 50%–75 % of 10 s window, 4) the amplitude > than 10 cm for more than 75 % of 10 s window. Regarding the resting tremor, the modulus of the peak value of the x-component of the angular velocity ($|r_{x,peak}|$) is considered to assign scores to the samples since it takes into account the amplitude and intensity of the tremor; in detail, if the $|r_{x,peak}|$ is lower than 10 dps over the whole exercise, the *Score 0* is assigned; if $|r_{x,peak}|$ is between 10 and 50 dps, *Score 1* is assigned; if $|r_{x,peak}|$ is between 50 and 100 dps, the *Score 2* is assigned, whereas if it is between 100 and 200 dps, a *Score 3* is assigned; finally, if *Score 4* is higher than 200 dps, a *Score 4* is assigned.

The tremor classification algorithm operates by dividing the 10s observation window into 4 windows of 2.5s each. An ML algorithm was developed to evaluate tremors on each window and assign a weight (w_i) based on intensity and persistence. Based on the weights of each window, the overall assessment is extracted, as described below. The dataset was constituted by collecting piezoelectric and inertial data tremors from patients with different scores; in detail, forty samples were collected for each class with a duration between 4 and 10s. After collecting and labeling the different movement samples, the dataset was split according to the 80 %/20 % ratio used to train and test a classification algorithm to score tremors on 2.5 s windows. This algorithm was deployed according to a processing chain reported in Fig. 7. In detail, 2.5 s time windows, with a 500 ms overlap, were employed to split the sample signals in frames. The processing chain involves extracting the spectral features of input signals; also, an 8th-order low-pass filter with an 8 Hz cut-off frequency was applied to remove unuseful components. Then, a NN with an input layer of 105 neurons, 3 dense layers of 70, 50, and 30 neurons, respectively, and an output layer of 5 classes (*Score 0*, *Score 1*, *Score 2*, *Score 3*, *Score 4*) was trained. Based on the tremor's amplitude, a score and a corresponding weight (w_i) were assigned to each window: 0 to *Score 0*, 1 to *Score 1*, 2 to *Score 2*, 3 to *Score 3*, and 4 to *Score 4* (Fig. 8a). The weights assigned in this way directly result from evaluating the tremor on the 2.5 s window; accumulating the weights enables evaluating the tremor persistence. Indeed, to assess the tremor's persistence and assign a final score over the entire 10 s window, the four scores obtained on 2.5 s windows (w_i) are added:

$$index = \sum_{i=1}^{4} w_i \tag{1}$$

Afterward, threshold values were applied to the cumulative index, which are a direct consequence of the previous scores' definition. For example, if a score of 2 is obtained on two windows (5 s) and a score of 0 on the remaining ones, the cumulative index will be 4, falling in the *Score 2* case. Thus, cumulative index values equal to 0, 1, 4, 9, and 16 can be derived for the five classes, consequently setting the threshold values according to the scores' definition. Based on the constancy requirements, a score from 0 to 4 is assigned according to the cumulative index on the 4 windows. If the inferring score assigned on the 2.5 s window does not exceed 0.5, a weight 999 (error code) is assigned, the test is stopped, and the patient is asked to redo the exercise (Fig. 8a). It was also necessary to assign a score to the intermediate indices: if the index is between 1 and 2, Score 1 is assigned; if the index is between 3 and 6, Score 2 is assigned; if the index is between 7 and 12, Score 3 is assigned; from index 13 onward, Score 4 is assigned (Fig. 8b).

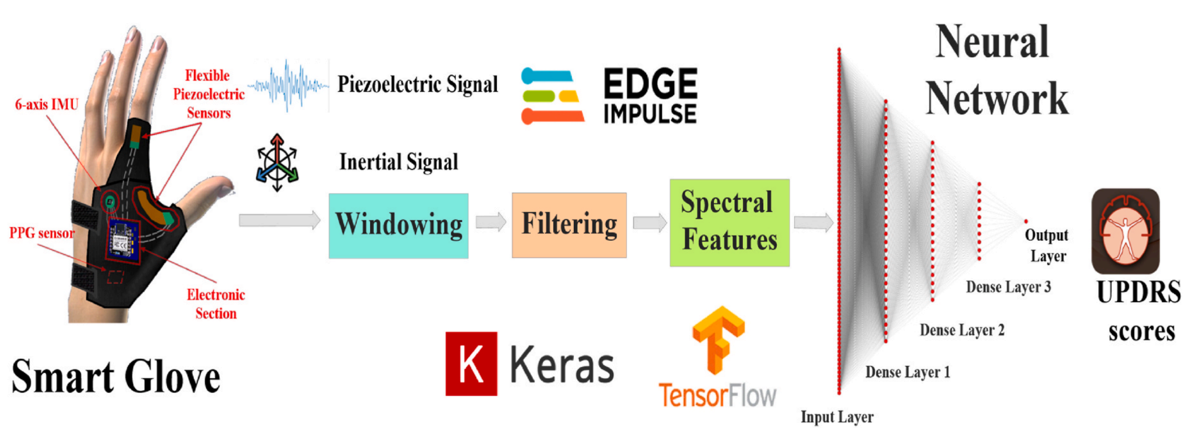

Fig. 7. Block diagram of the ML algorithm for Parkinson's disease evaluation.

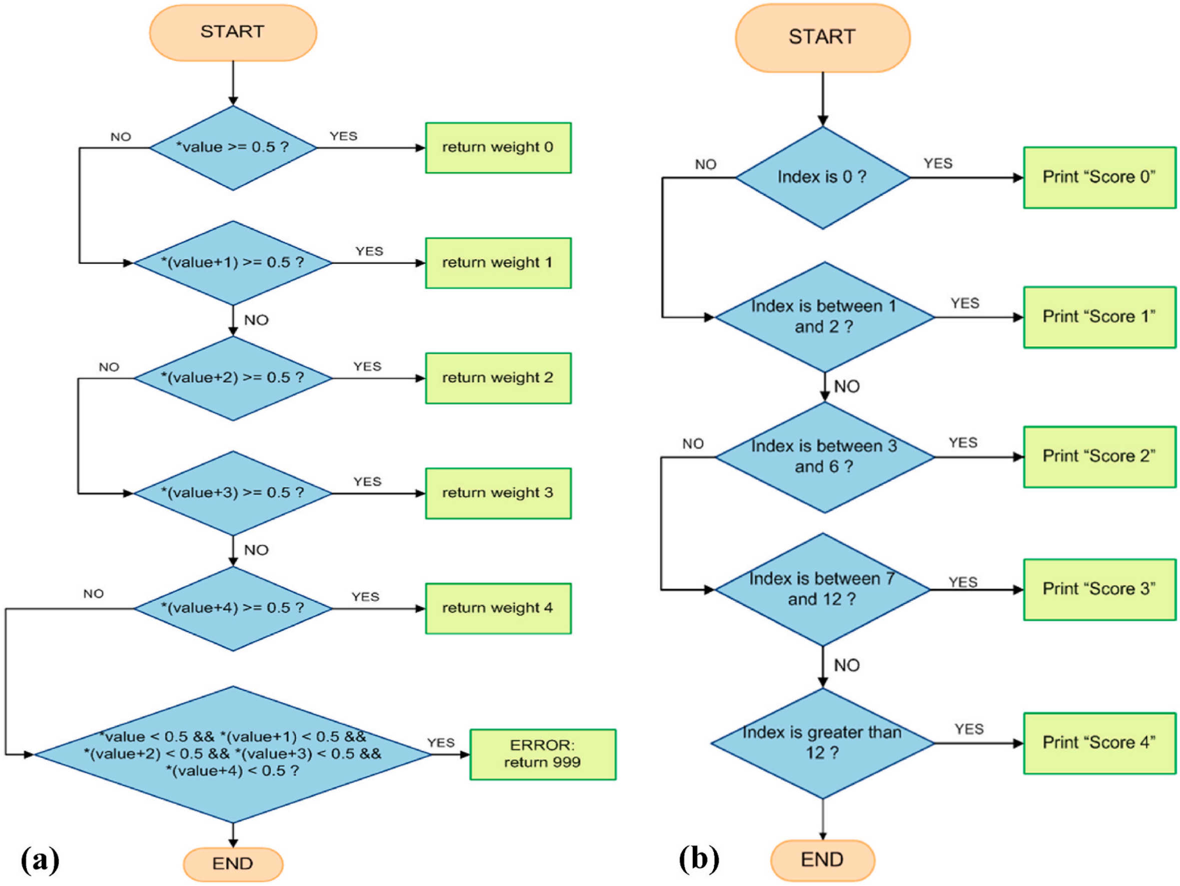

Fig. 8. Flowcharts of the methods to assign a weight to the scores assigned by the classification algorithm (**a**) and the score on the 10 s windows based on the cumulative index (**b**).

	SCORE 0	SCORE 1	SCORE 2	SCORE 3	SCORE 4	IDLE	UNCERTAIN
SCORE 0	100 %	0 %	0 %	0 %	0 %	0 %	0 %
SCORE 1	0 %	75 %	25 %	0 %	0 %	0 %	0 %
SCORE 2	0 %	0 %	100 %	0 %	0 %	0 %	0 %
SCORE 3	0 %	0 %	0 %	91.9 %	0 %	0 %	8.1 %
SCORE 4	0 %	0 %	0 %	0 %	97.5 %	0 %	2.5 %
IDLE	0 %	0 %	0 %	0 %	0 %	100 %	0 %
F1 SCORE	1.00	0.86	0.93	0.96	0.99	1.00	

(a)

	IDLE	SCORE 0	SCORE 1	SCORE 2	SCORE 3	SCORE 4	UNCERTAIN
IDLE	100 %	0 %	0 %	0 %	0 %	0 %	0 %
SCORE 0	0 %	100 %	0 %	0 %	0 %	0 %	0 %
SCORE 1	0 %	0 %	66.7 %	0 %	0 %	0 %	33.3 %
SCORE 2	0 %	0 %	0 %	100 %	0 %	0 %	0 %
SCORE 3	0 %	0 %	0 %	0 %	100 %	0 %	0 %
SCORE 4	0 %	0 %	0 %	0 %	0 %	100 %	0 %
F1 SCORE	1.00	1.00	0.80	1.00	1.00	1.00	

(b)

	SCORE 0	SCORE 1	SCORE 2	SCORE 3	SCORE 4	UNCERTAIN
SCORE 0	94.4 %	5.6 %	0 %	0 %	0 %	0 %
SCORE 1	3.0 %	97 %	0 %	0 %	0 %	0 %
SCORE 2	0 %	0 %	95.8%	4.2 %	0 %	0 %
SCORE 3	0 %	0 %	0 %	95.8 %	4.2%	0 %
SCORE 4	0 %	0 %	0 %	0 %	100 %	0 %
F1 SCORE	0.96	0.99	0.96	0.94	1.00	

(c)

Fig. 9. Confusion matrices of (**a**) finger-tapping model, (**b**) hand-fist closure model, and (**c**) tremor detection algorithm.

3.4. Performance of the developed models

This section reports the performance of the previously described ML algorithms for scoring the MDS-UPDRS-III exercises. In detail, Fig. 9 reports the confusion matrices related to the three ML algorithms described above obtained on the test set, comparing the predicted (columns) and actual classifications (rows), expressed as percentages of the test set support; it enables understanding where the model is making mistakes. The uncertain class is included in the predicted ones, indicating the condition in which the classifier cannot assign the samples to any class.

Several evaluation metrics are extracted from the confusion matrix to evaluate the models' performance, like accuracy, precision, recall, and F1-score. For each output class, TP (True Positive) indicates the positive samples correctly predicted, FN (False Negative) the samples actual positives that were incorrectly predicted as negative, and FP (False Positive) sample actual negatives that were incorrectly predicted as positive, and TN (True Negative) the samples correctly predicted as negative.

Thus, the metrics above are defined as:

$$Accuracy = \frac{TP + TN}{TP + TN + FP + FN} \tag{2}$$

$$Precision = \frac{TP}{TP + FP} \tag{3}$$

$$Recall = \frac{TP}{TP + FN} \tag{4}$$

$$F1 = 2 \bullet \frac{Precision \bullet Recall}{Precision + Recall} \tag{5}$$

For multi-class classification, the support-weighted average metrics were calculated by weighing the performance metrics for each class based on the support for that class in the test set. Also, ROC (Receiver Operating Characteristic) is a plot of the true positive rate (Recall) against the false positive rate (1 - Specificity) at various threshold levels. The AUC (Area Under the Curve) measures the classifier's performance; the closer it is to 1, the better the model distinguishes between positive and negative classes. Table 1 summarizes the performance of developed models in terms of accuracy, precision, recall, F1-score, and AUC calculated according to the support-weighted averaged definition.

4. Developed smart glove's firmware

The smart glove's firmware to asses Parkinson's stage is modular, i. e., the main code comprises three classification methods based on the ML models described above, called "*Hand Movement*", "*Finger Tapping*", and "*Tremor Detection*", respectively (Fig. 10). To start the evaluation, the patient must send a command related to the exercise to be carried out on the serial interface through Bluetooth. Once an admissible letter is received, the microcontroller launches the corresponding classification method. Also, heart rate and blood oxygenation readings were included in the code.

Once the assessment of the patient's condition is completed by means of the three tests for the movements evaluation and the acquisition of cardio-respiratory parameters (i.e., HR and SpO_2), the data are collected from the PC or smartphone in a JSON (Javascript Object Notification) package together with the timestamps related to the individual tests and forwarded to the cloud platform through the MQTT protocol. Medical consultations suggested that it was unnecessary for the acquisition of cardio-respiratory parameters to be synchronized with the evaluation tests of movements, given the objectives of the developed system.

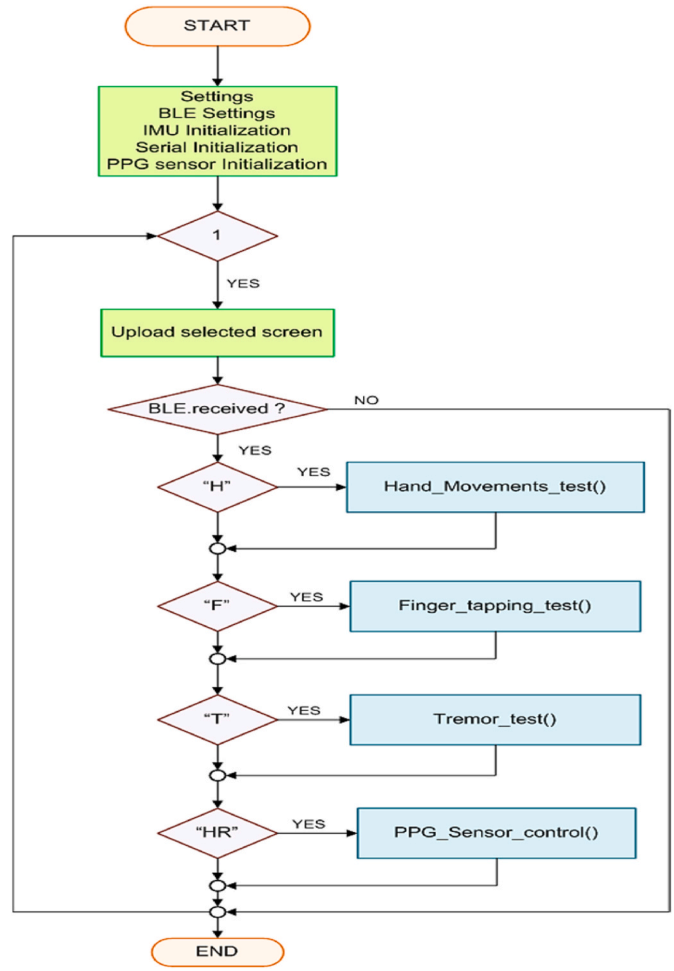

Fig. 10. Flowchart of the smart glove firmware to assess the PD severity.

Regarding the device's autonomy, experimental tests have been performed, demonstrating that during the executions of the different classification models, the average currents absorbed by the device are reported in Table 2. The measurements were carried out by a bench multimeter (model EDU34450A, manufactured by Keysight Technologies) placed in series to the power supply line, averaging the acquired current values over the measurement period.

The smart glove draws approximately 11.2 mA while acquiring and processing data from the MAX30102 sensor to measure HR and SpO_2. Furthermore, in idle conditions, the device is not engaged in any processing and consumes an average current of 10.1 mA. To optimize the

Table 1
Performance of the deployed ML algorithms.

Model	Accuracy [%]	Precision [%]	Recall [%]	F1-score [%]	AUC
Finger-Tapping	95.12	96.41	95.12	95.35	0.96
Hand-fist closure	98.39	98.59	98.39	98.59	0.98
Resting Tremor	96.62	96.69	97.08	96.57	0.98

Table 2
Mean current absorbed by the smart glove during the execution of the developed classification models.

Classification Model	Mean Absorbed Current [mA]
Finger-Tapping	32.2
Hand Movement	34.4
Resting Tremor	32.5

power consumption of the device when it is not involved in any processing, the System ON Low Power mode of the nRF52840 SoC was exploited, which allows to reduce the consumption of the device because the CPU is disabled, but the system remains partially active, allowing peripherals to continue working and wake up the CPU when it is necessary to start a new analysis. Consequently, the device's idle power consumption is reduced to 4.5 mA, extending its battery life significantly.

5. Discussions

From the results reported in the previous section, it is clear that the NN-based models perform excellently in evaluating the execution of the three exercises according to the MDS-UPDRS. Specifically, the model developed for finger-tapping evaluation achieves 95.12 % accuracy, 96.41 % precision, 95.12 % Recall, 95.35 % F1-score, and 0.96 AUC. Comparing the finger-tapping classification model reported in Ref. [24], which relies on inertial data and logistic regression, with the proposed ones, this last obtains a higher accuracy (95.12 % vs. 92.23 %). Also, in Ref. [25], different ML models were developed for evaluating finger-tapping based on 6-axis inertial data gathered by an electromagnetic tracking system (EMTS). The reported performance demonstrated that an SVM (Support Vector Machine) obtained 96 % accuracy, close to the performance of the classification models proposed in this paper (95.12 %). However, the results reported in Ref. [25] were obtained by offline processing and a pervasive acquisition system, hindering the patient's movements. Furthermore, the hand-fist closure model achieves excellent results, reaching 98.39 % accuracy, 98.59 % precision, 98.39 % recall, 98.59 % F1-score, and 0.98 AUC. The developed models for assessing resting tremors demonstrated optimal performance; indeed, the classification algorithm for evaluating the resting tremors over 2.5s windows reached 96.62 % accuracy, 96.69 % precision, 97.08 % recall, and 96.57 % F1-score over the test set; also, the detection over four consecutive windows enables evaluating the constancy of the tremor. Comparing its performance with similar algorithms reported in the literature, our system outperforms the multi-class classifier (XGBoost) reported in Ref. [26], which provides 70 % accuracy. Also, the reported classification algorithm performs better than that proposed in Ref. [27], which relies on an artificial neural network based on multilayer perceptron (ANN-MLP), obtaining 95.04 % accuracy.

The proposed smart glove is similar to other systems presented in the scientific literature; compared to them, the prototype glove integrates both piezoelectric and inertial sensors and thus combines data, providing a more detailed and comprehensive assessment of the Parkinson's disease severity; in contrast, the systems in Refs. [11,13] employ only one type of sensor to track the hand movements. Also, the proposed solution is discrete, non-invasive, and ready-to-use, not involving external acquisition and processing sections, unlike the works proposed [12]. In this context, the real strength of the proposed device is its ability to process, analyze, and classify data on-board the device itself without the need for an external elaboration section, unlike in systems in Refs. [11,13], providing the evaluation of the patient's condition directly. Compared with the smart glove presented in Ref. [15], our wearable device relies on custom piezoelectric sensors, which are less problematic (e.g., active sensor, higher sensitivity, fast response time) and more conformable than the piezoresistive ones. Furthermore, the proposed device includes fewer sensors than [15], collecting the information needed for staging the pathology severity. Also, our smart glove is based on embedded ML algorithms to classify the piezoelectric and inertial signals for evaluating the PD severity, not entrusting the processing local gateway as in Ref. [15]. Table 3 compares similar systems reported in the literature with the proposed one from the point of view of used sensor typology and number, application area, acquisition frequency and device, and available wireless connectivity.

6. Conclusions

The paper reports the development of a compact and ready-to-use smart glove to quantitatively monitor PD patients, combining advanced and commercial sensors as well as embedded ML algorithms. The device comprises highly flexible AlN-based piezoelectric transducers and an inertial sensor for detecting hand and arm movements during MDS-UPDRS-III tests. The glove comprises a low-power conditioning and processing section to elaborate and classify the acquired

Table 3
Comparison of similar systems reported in the literature for PD evaluation with the proposed one (N.A.: Not Available).

Work	Type of sensor	Sensor number	Application area	Evaluation method	Evaluation Scale	Acquisition frequency	Acquisition device	Wireless Connectivity
A. Vera et al. [7]	Triboelectric nanogenerator	1	Forearm	Finger-Tapping Hand-Opening-Closing Wrist Extension	MDS-UPDRS	N.A.	NRF5832	Bluetooth
J.-N. Kim et al. [9]	Biocompatible triboelectric nanogenerator	1	Wrist	Resting Tremor	Normal, Minor Tremor Sever Tremor	2 Hz–10 Hz	N.A.	N.A.
M. Heijmans et al. [10]	Inertial (accelerometer and gyroscope)	3	Wrist and chest	Resting Tremor	ESM score	200 Hz	N.A.	No
S. R. Sajal et al. [11]	Tri-axial accelerometer, voice recorder	1	In hand	Resting Tremor Voice modification	UPDRS	100 Hz	Smartphone	Wi-Fi
A. Batra et al. [13]	Metal ring with PVDF piezo transducer	1	Middle finger of the hand	Resting Tremor	N.A.	N.A.	Oscilloscope	No
M. Szumilas et al. [28]	Piezoelectric	2	Forearm	Resting Tremor	Average Pearson's distance	500 Hz	8-bit megaAVR microcontroller	No
M. Yousef et al. [12]	MEMS inertial	1	Wrist	Resting Tremor	N.A.	N.A.	Arduino Nano	Wi-Fi
S. Hosseini et al. [29]	Piezoelectric	2	Forearm	Resting Tremor	N.A.	N.A.	N.A.	N.A.
E. Khan et al. [30]	Piezoelectric pressure, inertial (MPU-6050)	N.A.	Hand	PD's unwanted hand movement	N.A.	N.A.	MSP430	N.A.
Developed smart glove	AlN flexible piezoelectric, PPG, inertial	2	At the index-thumb junction and on the index finger top	Finger-Tapping Hand-Movements Resting Tremor	MDS-UPDRS	45 Hz–51 Hz	nRF52840	BLE

signals. Also, three embedded ML algorithms based on NN were developed to classify the acquired piezoelectric and inertial data, each corresponding to standard tests, i.e., finger-tapping, hand gesture, and resting tremor. Datasets were collected from seven volunteers, six diagnosed with PD, and used to train and test the ML models. The test results indicated that developed embedded models obtained optimal performance, witnessed by the high obtained accuracy: 95.12 %, 98.39 %, and 96.62 % for finger-tapping, hand-fist closure, and resting tremor, respectively. The comparative analysis demonstrated that the proposed smart glove overcomes similar solutions in terms of performance and completeness.

CRediT authorship contribution statement

R. De Fazio: Writing – original draft, Software, Investigation, Data curation, Conceptualization. **C. Del-Valle-Soto:** Writing – original draft, Validation, Software, Data curation. **V.M. Mastronardi:** Writing – original draft, Validation, Investigation, Data curation. **M. De Vittorio:** Writing – review & editing, Writing – original draft, Validation, Supervision, Methodology, Conceptualization. **P. Visconti:** Writing – review & editing, Writing – original draft, Validation, Supervision, Investigation, Conceptualization.

Declaration of competing interest

The authors declare the following financial interests/personal relationships which may be considered as potential competing interestsNo financial interests/personal relationships to declare.

References

[1] C. Váradi, Clinical features of Parkinson's disease: the evolution of critical symptoms, Biology 9 (2020) 1–13.
[2] R. De Fazio, M. De Vittorio, P. Visconti, A BLE-connected piezoresistive and inertial chest band for Remote monitoring of the respiratory activity by an android application: hardware design and software optimization, Future Internet 14 (2022) 1–23.
[3] R. De Fazio, V.M. Mastronardi, M. Petruzzi, M. De Vittorio, P. Visconti, Human–machine interaction through advanced haptic sensors: a piezoelectric sensory glove with edge machine learning for gesture and Object recognition, Future Internet 15 (2023) 1–42.
[4] S. Spasojević, T.V. Ilić, I. Stojković, V. Potkonjak, A. Rodić, J. Santos-Victor, Quantitative assessment of the arm/hand movements in Parkinson's disease using a wireless armband device, Front. Neurol. 8 (2017) 1–15.
[5] J.C. van den Noort, R. Verhagen, K.J. van Dijk, P.H. Veltink, M.C.P.M. Vos, R.M. A. de Bie, et al., Quantification of hand motor symptoms in Parkinson's disease: a proof-of-principle study using inertial and force sensors, Ann. Biomed. Eng. 45 (2017) 2423–2436.
[6] Z. Lin, Y. Xiong, G. Cai, H. Dai, X. Xia, Y. Tan, et al., Quantification of parkinsonian bradykinesia based on axis-angle representation and SVM multi-class classification method, IEEE Access 6 (2018) 26895–26903.
[7] D.F. Vera A, T. He, J.-M. Redoute, C. Lee, M.R. Yuce, Flexible forearm triboelectric sensors for Parkinson's disease diagnosing and monitoring. 2022 44th Annu. Int. Conf. IEEE Eng. Med. Biol. Soc. EMBC, IEEE, Glasgow, Scotland, United Kingdom, 2022, pp. 4909–4912.
[8] D. Vera A, M.R. Yuce, Stretchable triboelectric sensor for measurement of the forearm muscles movements and fingers motion for Parkinson's disease assessment and assisting technologies, Med, Devices Sens 4 (2021) 1–12.
[9] J.-N. Kim, J. Lee, H. Lee, I.-K. Oh, Stretchable and self-healable catechol-chitosan-diatom hydrogel for triboelectric generator and self-powered tremor sensor targeting at Parkinson disease, Nano Energy 82 (2021) 1–12.
[10] M. Heijmans, J. Habets, M. Kuijf, P. Kubben, C. Herff, Evaluation of Parkinson's disease at home: predicting tremor from wearable sensors. 2019 41st Annu. Int. Conf. IEEE Eng. Med. Biol. Soc. EMBC, IEEE, Berlin, Germany, 2019, pp. 584–587.
[11] M.d.S.R. Sajal, M.d.T. Ehsan, R. Vaidyanathan, S. Wang, T. Aziz, K.A.A. Mamun, Telemonitoring Parkinson's disease using machine learning by combining tremor and voice analysis, Brain Inform 7 (2020) 1–12.
[12] M. Yousef, M. Hafizh, S. Sassi, G. Adeli, Development of a wearable wireless sensing device for characterization of hand tremors through vibration frequency analysis, J. Vib. Eng. Technol. 11 (2022) 3109–3120.
[13] A. Batra, J. Sampson, M. Aggarwal, A. Vaseashta, K. Grover, Wearable smart sensor ring to monitor the severity of hand tremor, Sens. & Trans. 253 (2021) 44–46.
[14] Y. Li, J. Yin, S. Liu, B. Xue, C. Shokoohi, G. Ge, et al., Learning hand kinematics for Parkinson's disease assessment using a multimodal sensor glove, Adv. Sci. 10 (2023) 1–10.
[15] V. Ravichandran, S. Sadhu, D. Convey, S. Guerrier, S. Chomal, A.-M. Dupre, et al., iTex gloves: design and in-home evaluation of an E-textile glove system for tele-assessment of Parkinson's disease, Sensors 23 (2023) 1–20, https://doi.org/10.3390/s23062877.
[16] L. Natta, F. Guido, L. Algieri, V.M. Mastronardi, F. Rizzi, E. Scarpa, et al., Conformable AlN piezoelectric sensors as a non-invasive approach for swallowing disorder assessment, ACS Sens. 6 (2021) 1761–1769.
[17] M. Mariello, L. Fachechi, F. Guido, De Vittorio M. Conformal, Ultra-thin skin-contact-actuated hybrid piezo/triboelectric wearable sensor based on AlN and parylene-encapsulated elastomeric blend, Adv. Funct. Mater. 31 (2021) 1–19.
[18] C.G. Goetz, B.C. Tilley, S.R. Shaftman, G.T. Stebbins, S. Fahn, P. Martinez-Martin, et al., Movement disorder society-sponsored revision of the unified Parkinson's disease rating scale (MDS-UPDRS): scale presentation and clinimetric testing results, Mov. Disord. 23 (2008) 2129–2170.
[19] L. Natta, P. Lombardi, V.M. Mastronardi, F. Guido, A. Qualtieri, M. Di Rienzo, et al., Flexible Piezoelectric Sensor with Integrated Electromagnetic Shield, US 2022/0416148 A1, 2022.
[20] P. Mailankody, M. Netravathi, P.K. Pal, Review of tremor in Parkinson's disease and atypical parkinsonian disorders, Neurol. India 65 (2017) 1083–1090.
[21] R. Bhidayasiri, P. Martinez-Martin, Chapter six - clinical assessments in Parkinson's disease: scales and monitoring, in: K.P. Bhatia, K.R. Chaudhuri, M. Stamelou (Eds.), Int. Rev. Neurobiol., vol. 132, Academic Press, 2017, pp. 129–182.
[22] F.A. Scorza, A.C. Fiorini, C.A. Scorza, J. Finsterer, Cardiac abnormalities in Parkinson's disease and Parkinsonism, J. Clin. Neurosci. 53 (2018) 1–5.
[23] K.G. Heimrich, T. Lehmann, P. Schlattmann, T. Prell, Heart rate variability analyses in Parkinson's disease: a systematic review and meta-analysis, Brain Sci. 11 (2021) 1–19.
[24] J. Stamatakis, J. Ambroise, J. Crémers, H. Sharei, V. Delvaux, B. Macq, et al., Finger tapping clinimetric score prediction in Parkinson's disease using low-cost accelerometers, Comput. Intell. Neurosci. 2013 (2013) 1–13.
[25] H. Dai, G. Cai, Z. Lin, Z. Wang, Q. Ye, Validation of inertial sensing-based wearable device for tremor and bradykinesia quantification, IEEE J. Biomed. Health Inform 25 (2021) 997–1005.
[26] A. Channa, O. Cramariuc, M. Memon, N. Popescu, N. Mammone, G. Ruggeri, Parkinson's disease resting tremor severity classification using machine learning with resampling techniques, Front. Neurosci. 16 (2022) 1–17.
[27] G. AlMahadin, A. Lotfi, M.M. Carthy, P. Breedon, Enhanced Parkinson's disease tremor severity classification by combining signal processing with resampling techniques, SN Comput. Sci. 3 (2021) 1–21.
[28] M. Szumilas, K. Lewenstein, E. Ślubowska, Verification of the functionality of device for monitoring human tremor, Biocybern. Biomed. Eng. 35 (2015) 240–246.
[29] S.M. Hosseini, H. Kalhori, A. Al-Jumaily, Active vibration control in human forearm model using paired piezoelectric sensor and actuator, J. Vib. Control 27 (2021) 2231–2242.
[30] E. Khan, A. Panchal, Mechanical movement aid to nerve damaged and Parkinson's using pressure & frequency detection (pseudo arm controller), Int. Conf. Commun. Signal Process. ICCSP, Melmaruvathur, India 158 (2015) 1544. IEEE; 2015.